frontiers | Frontiers in Physics

TYPE Mini Review
PUBLISHED 09 November 2022
DOI 10.3389/fphy.2022.1054234

OPEN ACCESS

EDITED BY
Bernard Gelloz,
Nagoya University, Japan

REVIEWED BY
Saikiran Vadavalli,
Gandhi Institute of Technology and Management (GITAM), India
Quan Sheng,
Tianjin University, China

*CORRESPONDENCE
Xuezong Yang,
xuezong.yang@ucas.ac.cn

SPECIALTY SECTION
This article was submitted to Optics and Photonics, a section of the journal Frontiers in Physics

RECEIVED 26 September 2022
ACCEPTED 26 October 2022
PUBLISHED 09 November 2022

CITATION
Liu Y, You W, Zhu C, Li M, Sun Y, Yin X, Chen D, Feng Y, Chen W and Yang X (2022), A review of ns-pulsed Raman lasers based on diamond crystal. *Front. Phys.* 10:1054234. doi: 10.3389/fphy.2022.1054234

A review of ns-pulsed Raman lasers based on diamond crystal

Yuxuan Liu[1,2], Wei You[1,2], Chengjie Zhu[1,2], Muye Li[2], Yuxiang Sun[2], Xiongfei Yin[2], Dijun Chen[1,2], Yan Feng[1,2], Weibiao Chen[1,2] and Xuezong Yang[2]*

[1]Shanghai Institute of Optics and Fine Mechanics, Chinese Academy of Sciences, Shanghai, China, [2]Hangzhou Institute for Advanced Study, University of Chinese Academy of Sciences, Hangzhou, China

High-power ns-pulsed lasers have been widely used in many significant applications, including laser radar, remote-sensing, biomedicine, industrial process, and military defense. Stimulated Raman scattering (SRS) provides an efficient method for extending the wavelengths of laser radiation. Due to the excellent thermal conductivity, high damage threshold, and high gain coefficient, diamond crystal is considered the most potential SRS material to address laser output in specific wavelength regions with high power, high beam quality, and high conversion efficiency. This paper reviews the advances of ns-pulsed crystalline Raman lasers and particularly emphasizes the progress of ns-pulsed diamond Raman lasers (DRLs) in the past decade. DRL has demonstrated a maximum peak power of 1.2 MW at 1.240 μm with a pulse duration of 8 ns. It can also generate high-energy ns pulses featuring Fourier-limited spectral linewidth. The superior optical characteristics and the mature technology of synthetic diamond crystal will make DRL a promising technique to achieve higher performance ns laser pulses.

KEYWORDS

ns-pulsed diamond Raman laser, solid-state laser, stimulated Raman scattering, high energy, wavelength expansion

Introduction

The importance of ns-pulsed lasers are indisputable due to their wide use in the fields of range finding [1], laser radars [2, 3], molecular biology [4], laser processing [5], and remote sensing [6]. Furthermore, high-power ns-pulsed lasers play an important role in specific wavelength requirements, such as remote sensing of sodium layer at 0.589 μm [7–9], underwater laser communication using blue-green light [10], tropospheric ozone detection at 0.285 and 0.291 μm [11] and wind velocity measurement at “eye-safe” 1.5 μm [12]. Currently, the crucial technologies for expanding the wavelength of ns-pulsed laser include optical parametric oscillation (OPO), second-harmonic generation, sum- and difference-frequency generation, and stimulated Raman scattering (SRS).

SRS as an essential third-order nonlinear effect is a general but efficient technology to expand the laser wavelength. Raman media have gain for all transmitted bands and thus the output wavelength extension is associated with the incident pump and the cascade Stokes cavity design. Noteworthy, the property of no-spatial hole burning of Raman gain makes the output light more inclined to operate with single longitudinal mode (SLM). Furthermore, compared to OPO, the automatic phase-matching of SRS laser has no necessity for angle or temperature tuning. At present, ns-pulsed Raman lasers are mainly based on ionic bonds Raman crystals, such as tungstate, nitrate and vanadate crystals. An output pulse energy of 10 mJ in an external resonator $PbWO_4$ Raman laser has been achieved with a maximum conversion efficiency of 24% and a pulse width of 20 ns at the first Stokes [13]. $Ba(NO_3)_2$ Raman laser has been demonstrated to realize an output energy of 250 mJ at its first-Stokes wavelength of 1.178 μm, and obtain a 90 mJ output at 0.589 μm with the pulse width of 1.5 ns after frequency doubling [14]. Moreover, an intracavity YVO_4 Raman laser at 1.176 μm with 1.67 mJ output energy and 8.8% conversion efficiency has been reported [15]. Although those above-mentioned Raman lasers have been proven as mature technology to generate high-power ns-pulsed laser, they manifest a profound thermal lens effect which consequently restricts further power promotion and even leads to beam deterioration and crystal damage. Besides, the relatively small Raman phonon vibration frequency of those crystals leads to complicated optical device design, usually based on the cascaded SRS process to access the required output wavelength.

Single-crystal diamond is an excellent crystalline Raman material with superior properties [16], such as preeminent thermal conductivity, high damage threshold, high Raman gain coefficient and the maximal Raman frequency shift. With these extraordinary characteristics, a considerable amount of literature has been published on diamond Raman lasers (DRLs) in the last decade. The remarkable achievements of DRLs have been incorporated into various Raman laser formats, including deep UV [17], visible [18–23], NIR [24–30] and MIR [31] wavelengths in continuous wave (CW) [32], quasi-CW (QCW) [28–30] and pulsed [18, 22, 24–26, 33–37] regimes. For the ns-pulsed DRL, maximum pulse energy of 9 mJ at 1.240 μm with pulse width of 8 ns and conversion efficiency of 24% has been reported by Robert J. Williams at Macquarie University [38].

In this paper, we summarize the development of ns-pulsed DRLs that have been explored over the past decade. Firstly, we detail the comparison of diamond and other Raman crystals about their optical and physical properties. The subsequent sections review the development stages of ns-pulsed DRLs operating near quantum limit, wide wavelength coverage, single frequency operation, beam brightness enhancement and microcavity resonator. Lastly, we discuss the current limitations and the further steps of the ns-pulsed DRLs.

Superior properties of diamond crystal

With the development of crystal-growth technology, many crystalline Raman mediums, including YVO_4, $BaWO_4$, $Ba(NO_3)_2$ and diamond, become commercially available and the attained Raman lasers move to a mature stage. The choice standards or central characteristics of Raman crystal for SRS laser performance rest on a combination of factors, including Raman mode shift, Raman gain coefficient, transmission spectrum, crystal damage threshold and thermal conductivity. Some representative optical and physical properties of common Raman crystals are detailed in Table 1. According to Table 1, diamond crystal shows many distinguished optical and thermal properties. The main properties of diamond with some common crystalline Raman materials are outlined below.

Wide transmission spectrum

Diamond has the widest spectrum transmittance among all the Raman crystals. Except for the UV-edge absorption (λ < 0.225 μm) and the infrared lattice absorption in the range of 2.6–6.2 μm, diamond possesses high transmittance in the spectrum range from 0.23 to 100 μm [16]. Furthermore, combined with the widest transparent region and the largest crystalline Raman shift 1332.3 cm^{-1}, the output wavelength of DRLs can be greatly expanded by means of a cascaded SRS process.

Preeminent thermal characteristics

The thermal dissipation capacity for many Raman crystals must be taken into account since it impacts markedly on the Raman laser power scaling. When the heat deposited in the Raman crystal is unable to dissipate promptly, the negative thermal effects such as thermal lensing and birefringence will occur, destabilizing the laser resonator and then restricting the laser beam quality, output power and conversion efficiency [42]. The CVD-grown single diamond crystal has been measured to have a record-high thermal conductivity (2000 W/m K), two to three orders of magnitude higher than other conventional Raman crystals, and an extremely low thermal expansion coefficient (1.1×10^{-6} K^{-1}), at least four times lower than other crystals [16, 43].

High damage threshold

The high Raman gain (10–16 cm/GW at 1 μm [24]) and the superior thermal characteristics make diamond promising for generating high-power ns-pulsed Raman laser. The pivotal

TABLE 1 Optical and physical properties of some of common Raman crystals [16].

Materials	$PbWO_4$	$BaWO_4$	$Ba(NO_3)_2$	YVO_4	Diamond
Raman gain coefficient[a] (cm/GW @ 1 μm)	3.1	8.5	11	4.5	10–16
Optical transparency[a] (μm)	0.33–5.5	0.26–5	0.35–1.8	0.4–5	>0.23
Raman shift[a] (cm^{-1})	901, 323	925	1047.6	890	1332.5
Refractive index[a] @1 μm	2.15	1.84	1.56	1.96	2.39
Raman linewidth FWHM[a] (cm^{-1})	4.3	1.6	0.4	3	1.5
Thermal conductivity[a] (W/m·K)	—	3	1.17	5.2	2000
Thermal expansion[a] ($\times10^{-6}$ K^{-1})	—	4–6	18.2	4.43	1.1
Surface damage threshold[a] uncoated (GW/cm^2)	~0.25 [39] at 0.532 μm	—	~0.34 [40] at 0.532 μm	—	2 [41] at 0.532 μm 8 [41] at 1.064 μm

[a]At room temperature.

limitation of pulse energy increase is the surface damage threshold of gain crystal. Compared to the reported damage threshold of $PbWO_4$ (~0.25 GW/cm^2) [39] and $Ba(NO_3)_2$ (~0.4 GW/cm^2) [40] at 0.532 μm, uncoated diamond crystal has a much higher surface damage threshold of 2 GW/cm^2 at 0.532 μm and 8 GW/cm^2 at 1.064 μm, which manifests the potential of diamond crystal to address high-power ns-pulsed Raman laser. For ns-pulsed DRLs, damage-free operation was achieved experimentally when the intracavity accepted approximately 300 MW/cm^2 incident pump (1.064 μm, 10-ns pulse width) and similar first Stokes (1.240 μm) intensity. When the resonator was designed to mainly output the second Stokes at 1.485 μm (the output coupling at the first Stokes < 2%), only the anti-reflection coatings damage of diamond was observed and the intracavity intensity was about 1 GW/cm^2 (including pump and Stokes energy) [41].

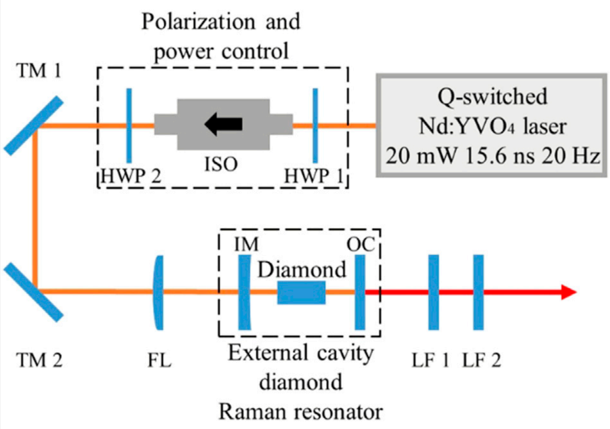

FIGURE 1
The experimental setup in [25]. HWP, half-wave plate; ISO, optical isolator; TM, turning mirror; FL, focus lens; IM, input mirror; OC, output coupler; LF, long-pass filter. Image originally published in Ref. [25] and reproduced with permission from IOP Publishing.

Ns-pulsed diamond Raman lasers operating near the quantum limit

The slope efficiency defined as the slope of the curve obtained by plotting the laser output power versus the pump power is a crucial index to evaluate the Raman laser performance, since it is determined by comprehensive factors of the resonator, including bulk absorption loss, Raman quantum defect, the output coupling of the laser resonator and so on. Due to the commercialization of high-quality single-crystal diamond, DRLs have shown near quantum-limited high slope efficiency [24, 25].

In 2010, Alexander Sabella et al. from Macquarie University achieved a 1.240 μm diamond Raman laser operating near the quantum limit [24]. The pump source was a linearly polarized Q-switched Nd: YAG laser operating at the center wavelength of 1.064 μm with maximum output energy of 0.9 mJ and pulse repetition of 5 kHz. The Raman medium was a 6.9-mm-long anti-reflection (AR) coated, Type IIa single diamond crystal (Element Six, United Kingdom). To access the maximum Raman gain, the pump polarization direction was rotated parallel to the <111> axis in diamond. The maximum conversion efficiency was 61% for the first Stokes and 65% for the total (first and second) Stokes. Before the second Stokes generation, the slope efficiency was 84%, which is near the quantum efficiency of 85.8%. The gap between the experimental slope efficiency and the quantum efficiency was owing to the parasitic losses. To maintain a near-quantum slope efficiency of DRL at the first Stokes, the generation of second Stokes must be suppressed. The most effective way is to optimize the input and output coupler coatings. Hence, Yao Wang et al. from China Academy of Engineering Physics, studied the relationship between cavity coupling and their output characteristics in 2020 [25]. The experimental setup is similar to the reference [24] shown in Figure 1.

TABLE 2 Summaries of ns-pulsed DRLs operating near the quantum limit.

References	Pump laser	Raman crystal (length)	Output wavelength (μm)	Output power (mJ)	Slope efficiency (%)	Maximum conversion efficiency (%)	Year
[24]	Q-switched Nd:YAG: 1.064 μm, 5 kHz	Diamond (6.9 mm)	1.240	0.4 (8 ns)	84	61	2010
[25]	Q-switched $Nd:YVO_4$: 1.0644 μm, 20 Hz	Diamond (7 mm)	1.2403	0.26 (10 ns)	84.3	32.2	2020

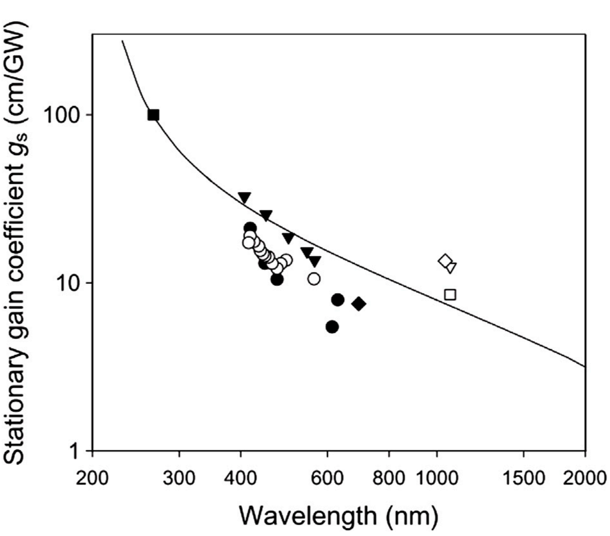

FIGURE 2
Stationary gain coefficient as a function of pump wavelength. Reference to the data points are summarized in Ref. [44]. The curve using Equations (1.13), (1.14) and (1.20) in Ref. [44].

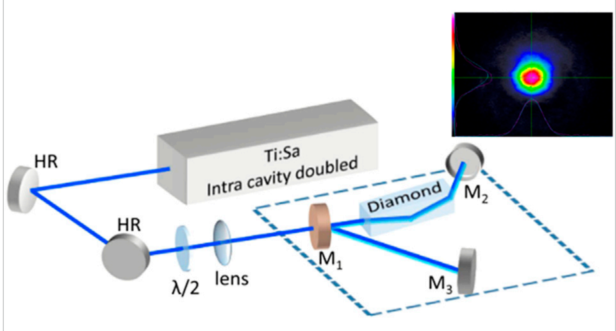

FIGURE 3
Schematic layout and beam spatial profile of Ref. [46]. HR, high reflect mirror; Mx, mirror. Image originally published in Ref. [46] and reproduced with permission according to the open access licenses © [2019] Optica Publishing Group under the terms of the Optica Open Access Publishing Agreement.

In this experiment, a homemade Q-switched Nd: YVO4 laser with a maximum pulse energy of 1 mJ at 1.0644 μm was used as the pump source for the external cavity DRL. The maximum output pulse energy of the first Stokes was 0.26 mJ with the incident pump of ~0.8 mJ, and the slope efficiency was 84.3%, which was higher than that in [24] and closer to the quantum limit of 85.8%. However, non-optimal transmittance of cavity mirrors and the intracavity wastage led to a much lower conversion efficiency of 32.2% compared to 61% in Ref. [24]. In the next experiment, an input mirror with lower transmission (20%) at 1.485 μm was used to replace the original one and the first Stokes and the second Stokes were generated simultaneously. The maximum output pulse energy of total Raman energy was 0.44 mJ (the first and the second Stokes was 0.26 and 0.18 mJ, respectively) at the maximum pump level (~0.9 mJ) with the slope efficiency of 73%, which was the highest slope efficiency in dual-wavelength external cavity DRLs. Besides, the total conversion efficiency was increased to 49%. The results of ns-pulsed DRLs operating near the quantum limit are briefly reviewed in Table 2.

Wavelength expansion of ns-pulsed diamond Raman lasers

Due to the wide transparent region, ns-pulsed DRLs are able to realize visible, NIR or MIR operation. Besides, the high Raman gain of diamond in different bands supports the efficient output wavelength extension. The stationary gain coefficient of visible and NIR bands is summarized in Ref. [44] (Figure 2). For typical wavelengths, diamond Raman gain coefficient is about 75 cm/GW [45] at 0.532 μm and 10–16 cm/GW [24] at 1 μm.

Katerina Chrysalidis et al. from CERN have demonstrated an efficient and high beam quality visible ns-pulsed DRL with stable linewidth of 5 GHz and continuously tunable wavelength from 0.475 to 0.5 μm [46]. An 8-mm-long CVD-grown single crystal was placed at an angle of 10° with respect to the resonator mode to avoid etalon effects introduced by the uncoated Raman medium. The schematic layout and beam spatial profile are shown in Figure 3. The large tunability and stable linewidth

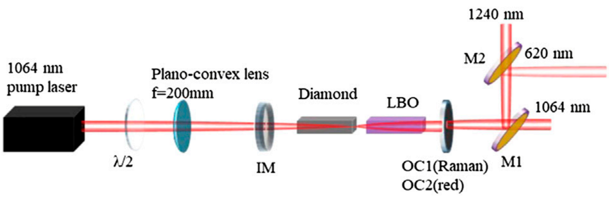

FIGURE 4
The experimental setup in Ref. [47]. IM, input mirror; OC, output coupler; M, mirror. Image originally published in Ref. [47] and reproduced with permission from Springer Nature.

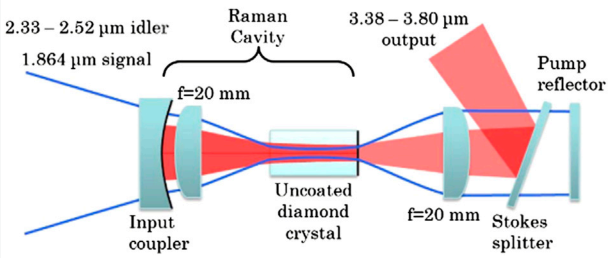

FIGURE 6
Layout of the diamond Raman laser in Ref. [31]. Image originally published in Ref. [31] and reproduced with permission from Optica Publishing group © The Optical Society.

in the GHz range were mainly designed for resonance laser ionization. In 2009, R. P. Mildren and A. Sabella used a 6.7-mm-long Brewster-cut diamond crystal to realize a 0.237 mJ output external cavity DRL at 0.573 µm with 5 kHz repetition rate and 6.5 ns FWHM pulse duration [21]. The conversion and slope efficiency were 63.5% and 75%, respectively. Recently, ns-pulsed DRLs at visible region using internal cavity frequency doubling technology has been demonstrated. An intracavity frequency double pulsed DRL emitting at 0.620 µm with 0.15 mJ output energy, 11% conversion efficiency and 5 kHz repetition rate was designed by Yilan Chen et al. [47] and the experimental setup is shown in Figure 4.

Since light longer than ~1.4 µm is strongly absorbed in the eye's cornea and lens and thus the retina of the eyes will keep away from damage, plenty of ns-pulsed DRLs at the "eye-safe range" have been reported. In 2014, Aaron McKay et al. used an 8-mm-long AR-coated diamond and achieved 0.46 mJ s Stokes (1.485 µm) and 40% conversion efficiency with a high repetition of 35 kHz [35]. Moreover, M. Jelinek, Jr et al. from Czech Technical University achieved a wavelength of 1.63 µm external cavity DRL with 0.047 mJ and 6 ns pulse duration [48]. For higher energy pursuit, in 2018, Robert J. Williams et al. developed the highest output energy of 9.7 mJ at 1.240 µm, to the best of our knowledge, in a flat-flat cavity DRL with 24.5% energy conversion efficiency, 46% slope efficiency and high beam quality [38].

Due to the infrared lattice absorption in the range of 2.6–6.2 µm, the extension of DRLs to MIR wavelength is challenging. In 2019, Giorgos Demetriou, Alan J. Kemp and Vasili Savitski from the Institute of Photonics reported a 1.67 mJ output DRL operating at 2.52 µm with 38% conversion efficiency and 11–15 ns pulse duration [49], and the layout of the experimental setup is shown in Figure 5. Due to the practical application of plastics processing, this work proved the feasibility of DRLs at the wavelength of MIR.

Furthermore, the multiphoton absorption bands of diamond (2.6–6.2 µm) are much narrower than silicon (6–30 µm), making diamond an alternative to silicon. In 2014, Alexander Sabella et al. from Macquarie University reported a tunable MIR DRL operating from 3.38 to 3.80 µm by varying the OPO pump wavelength, which was the longest wavelength in solid-state Raman laser to our knowledge [31]. A delicate structure depicted in Figure 6 is designed. The maximum Stokes output

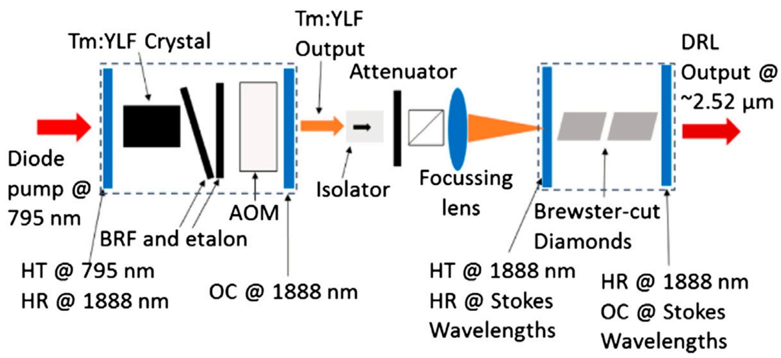

FIGURE 5
Layout of the experimental setup in Ref. [49]. Image originally published in Ref. [49] and reproduced with permission according to the open access licenses © [2019] Optica Publishing Group under the terms of the Optica Open Access Publishing Agreement.

TABLE 3 Summary of DRLs for wavelength expansion.

References	Pump laser	Repetition rate (Hz)	Raman crystal (length)	Output wavelength (μm)	Output power (mJ)	Pulse width (ns)	Maximum conversion efficiency (%)	Year
[46]	Ti: Sapphire laser	10 k	Diamond (8 mm)	0.475–0.5	0.018	—	28	2010
[21]	Q-switched Nd:YAG 0.532 μm	5 k	Diamond (6.7 mm) brewster-cut	0.573	0.237	6.5	63.5	2009
[35]	Q-switched Nd: YVO_4 1.064 μm	35 k	Diamond (8 mm)	1.485	0.46	—	40	2014
[48]	Q-switched Nd:YAP 1.34 μm	—	Diamond (2 mm)	1.630	0.047	6	1.6	2012
[38]	—	5	Diamond (7 mm)	1.240	9.7	8	24.5	2018
[47]	Nd:YAG 1.064 μm	2 k	Diamond (7 mm)	0.620	0.375	~2.5	11	2022
[49]	Tm:LiYF4 1.89 μm	5	Diamond (4 mm + 5.6 mm) brewster-cut	2.52	1.67	11–15	38	2019
[31]	Littmann-Metcalf KTP OPO	10	Diamond (8 mm)	3.38–3.80	0.115	3–4	18	2014

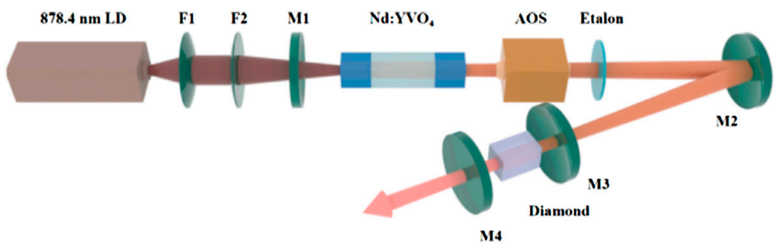

FIGURE 7
Diagram of the ns pulsed SLM DRL at 1.634 μm reported in Ref. [26]. LD, laser diode; F1 + F2, telescopic system; M, mirror; AOS, acousto-optic switch. Image originally published in Ref. [26] and reproduced with permission from Optica Publishing group © The Optical Society.

energy of 115 μJ was achieved by introducing a second pump at an anti-Stokes wavelength to initiate a seed at the Stokes by four waves mixing effect. This remarkable study provided a novel approach for MIR wavelength and even for the generation of wavelengths longer than 6 μm. The research mentioned above are concluded in Table 3.

Ns-pulsed diamond Raman lasers operating at single longitudinal mode

Due to the high pulse energy and narrow linewidth, ns-pulsed Raman lasers with flexible wavelengths are widely used in many crucial applications, such as coherent detection, high-resolution spectroscopy, laser isotope separation, and so on. Four typical techniques for obtaining SLM operation in DRLs were summarized in Ref. [50], including the non-spatial-hole-burning effect of Raman gain, cavity locking, intracavity nonlinear gain competition, and inserting mode selection elements. However, the SLM DRLs were all operating in CW or Q-CW [19, 32, 51–53].

Recently, Houjie Ma et al. from Guangdong Provincial Engineering Research Center of Crystal and Laser Technology demonstrated the first ns-pulsed SLM intracavity DRL operating at 1.634 μm pumped by a Q-switched 1.342 μm Nd: YVO_4 laser [26]. The experimental diagram is shown in Figure 7.

A 9-mm-long Raman cavity with a 6-mm-long diamond was designed to increase the cavity mode spacing to 8.6 GHz, which limited the number of oscillating modes. A 0.3-mm-thick etalon with fitness of 3.3 was inserted to realize the high power SLM operation. At the incident pump power of ~0.9 mJ, the highest SLM output power of 0.065 mJ was obtained with a pulse duration of ~9 ns and a spectral linewidth of ~77 MHz. In the same year, a monolithic diamond SLM resonator was demonstrated by Eduardo Granados et al. from CERN [22]. A tunable dye laser with a linewidth of 11.9 GHz was used as the pump source. In this experiment, the length of the monolithic diamond cavity was 5 mm, corresponding to the cavity-free

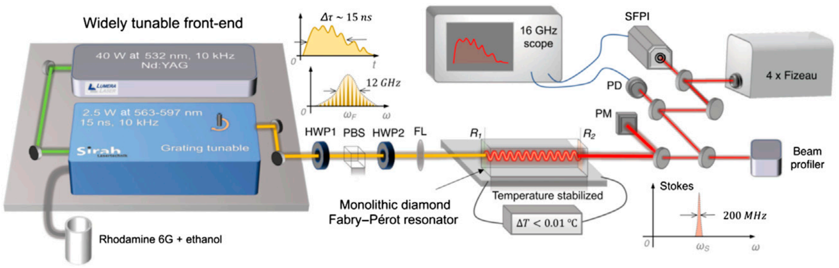

FIGURE 8
Experiment setup of the SLM monolithic diamond laser at 0.614 μm [22]. HWP, half-wave-plate; PBS, polarizing beam splitter; FL, focusing lens; PM, power meter; PD, photodiode; SFPI, scanning Fabry-Perot interferometer. Image originally published in Ref. [22] and reproduced with permission according to the open access licenses © [2022] Optica Publishing Group under the terms of the Optica Open Access Publishing Agreement.

TABLE 4 The review of SLM ns-pulsed DRLs.

References	Pump laser	Raman crystal (length)	Output wavelength (μm)	SLM power (mJ)	Maximum conversion efficiency	Spectral linewidth (MHz)	Year
[26]	Nd: YVO_4 1.342 μm, 25 kHz	Diamond (6 mm)	1.634	0.065	~7.3%	~77	2022
[22]	Dye laser 0.568 μm, 10 kHz	Diamond (5 mm)	0.614	~0.1	47%	~200	2022

spectral range (FSR) of 12 GHz, which was close to the linewidth of the dye pump laser. The schematic of the laser system was shown in Figure 8. The output linewidth of the SLM Stokes was ~200 MHz and the pulse energy was ~0.1 mJ with an energy conversion efficiency of 47%. The comparison of two ns-pulsed SLM DRLs is detailed in Table 4.

Beam brightness enhancement of ns-pulsed diamond Raman lasers

One of the most remarkable features of Raman lasers is the beam clean-up effect. This Raman beam clean-up feature is shown in the experiment as the beam quality factor (M^2) of Stokes is smaller than that of the incident pump beam due to the direct consequence of four-wave mixing and gain-guiding [54]. Two important parameters describing the beam quality of lasers are the beam quality factor M^2 and the brightness of beam B. They were defined as

$$M^2 = \frac{\omega \cdot \theta \cdot \pi}{4\lambda}, \ B = \frac{P}{\lambda^2 M_x^2 M_y^2}$$

where the ω is the beam waist diameter, θ is the beam divergence angle, P is the average power, λ is the wavelength, and M_x^2 and M_y^2 are the beam quality factors of two orthogonal axes [35]. The beam aberration, focus ability and beam intensity can be easily depicted by these parameters.

In the experiment of an efficient second Stokes external DRL at 1.485 μm, Alexander Sabella et al. demonstrated an ns-pulsed output with near diffraction-limited beam quality ($M^2 = 1.05$) pumped by an Nd:YAG laser with beam quality ($M^2 = 1.5$) [33]. In 2014, Aaron McKay *et al.* achieved simultaneous brightness enhancement and high conversion efficiency in an external cavity DRL [35]. The beam quality factors $M_{x,y}^2$ was 1.17 ± 0.08 for average output power up to 10 W, which was 2.7 times lower than the factor of the incident pump. The beam profiles of the pump and Raman are shown in Figure 9A. The brightness of input and output beams were 289.4 $MW \cdot Sr^{-1} \cdot cm^{-2}$ and 334.5 $MW \cdot Sr^{-1} \cdot cm^{-2}$, respectively, corresponding to a brightness enhancement of ~1.16. Although the pump beam quality was much worse than that in Ref. [33], a higher Stokes power of 16.2 W and similar conversion efficiency of 40% were achieved.

In comparison, for barium nitrate Raman crystal, though the positive lens was used to compensate the thermal lens effect, the beam quality factor was not improved and still approximate of 3 (shown in Figure 9B) at an average output power of 5.5W [55]. The low thermal conductivity and high thermal expansion of

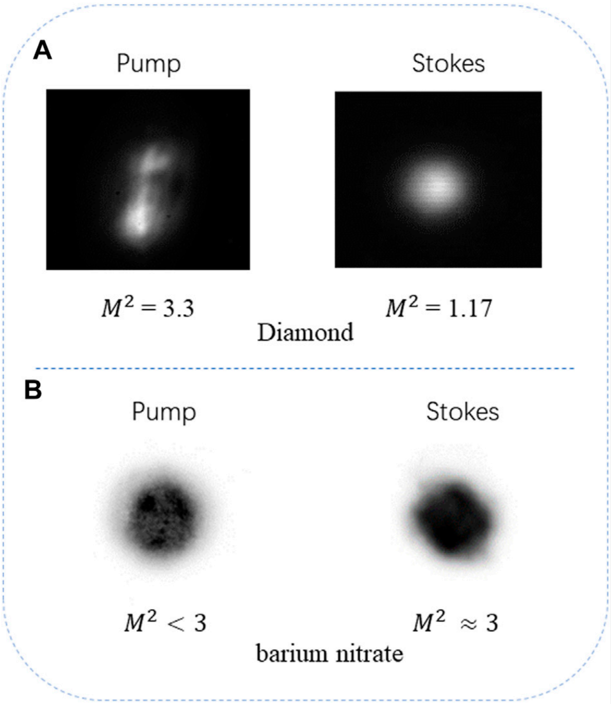

FIGURE 9
The beam profiles of pump and Raman lasers. **(A)** diamond Raman laser [35]; **(B)** Barium nitrate Raman laser [55]. Image **(A)** originally published in Ref. [35] and reproduced with permission from WILEY—VCH VERLAG GMBH & CO. Image **(B)** originally published in Ref. [55] and reproduced with permission from Springer Nature.

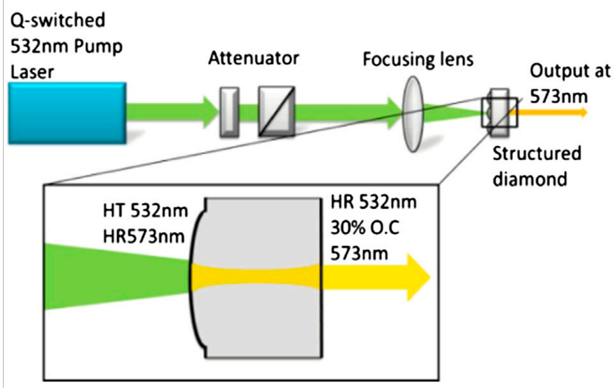

FIGURE 10
Schematic diagram of experimental setup in Ref. [56]. Image originally published in Ref. [56] and reproduced with permission from Optica Publishing group © The Optical Society.

molecular-ion Raman crystals lead to severe thermal induced beam distortion that may counteract the benefits from Raman beam cleanup effect [33]. The details of the above-mentioned references are shown in Table 5.

Microcavity ns-pulsed diamond Raman lasers

In comparison to the traditional resonator structure, the microcavity is beneficial to the simplification of cavity design, the compactness of laser structure, the suppression of mode-hopping and the implementation of SLM operation. In microcavity DRLs, the interior of the diamond crystal acts as the gain medium and the surfaces serves as the cavity mirrors, which signify a plane-plane resonant cavity is constituted only by a piece of diamond crystal.

Early in 2015, Sean Reilly et al. from University of Strathclyde has been experimentally demonstrated the feasibility of monolithic DRLs by comparing it to a plane-plane cavity [56]. The experiment results showed that the total output energy and conversion efficiency of the microcavity were 0.0134 mJ and 84%, respectively, which were higher than those in the plane-plane case. An array of spherical microlenses were etched on the incident surface of diamond with the purpose of reducing pump spot size. The schematic diagram is shown in Figure 10.

In 2021, Shihui Ma et al. from Tianjin University of Technology focused on the reflectance of the surfaces of diamond and the beam radiuses of pump, and reported a microcavity ns-pulsed second Stokes DRL constructed using a 6-mm-long diamond (supplied by Ningbo Institute of Material Technology & Engineering) as the Raman medium pumped by using a solid-state pulsed green laser (0.532 μm) with a repetition rate of 10 kHz and pulse width of 22 ns [18]. For the second Stokes output at 0.620 μm, an output power of 0.195 mJ and slope efficiency of 22.8% were obtained by optimizing the beam size of the incident pump and the reflectivity of the diamond output and input surfaces. The schematic of the diamond Raman

TABLE 5 The summary of brightness enhancement ns pulsed Raman lasers.

References	Repetition frequency (Hz)	Pump M^2	Raman crystal (length)	Output power (W)	Stokes M^2	B of Stokes ($MW \cdot Sr^{-1} \cdot cm^{-2}$)	Year
[33]	5 k	<1.5	Diamond (6.9 mm)	1.63	1.05	~67	2011
[35]	36 k	~3.3	Diamond (8 mm)	10	~1.17	334.5	2014
[55]	100	<3	$Ba(NO_3)_2$ (70 mm)	5.5	~3	23.9	2012

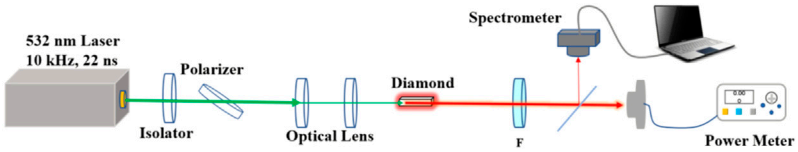

FIGURE 11
Schematic of the diamond Raman red laser in Ref. [18]. Image originally published in Ref. [18] and reproduced with permission from ELSEVIER BV.

TABLE 6 Summary of microcavity ns-pulsed DRLs.

Ref.	Pump laser	Repetition frequency (Hz)	Cavity length (mm)	Output wavelength (μm)	Output power (mJ)	Maximum conversion efficiency (%)	Pulse duration (ns)	Year
[56]	Elforlight SPOT laser 0.532 μm	10 k	2	0.573 (1st) 0.620 (2nd) 0.676 (3rd)	0.0134 (total)	84	—(1st) 1.6 (2nd) 0.9 (3rd)	2015
[18]	Solid-state pulsed laser 0.532 μm	10 k	6	0.620 (2nd)	0.195	15	2.1	2021
[22]	Dye laser 0.568 μm	10 k	5	0.614 (1st)	~0.1	47	15	2022

TABLE 7 The representative results of ns-pulsed DRLs.

Direction	Repetition frequency (Hz)	Output wavelength (μm)	Output power (mJ)	Maximum conversion efficiency	Slope efficiency	References
Quantum limit conversion	20	1.2403	0.26	32.3%	84.3%	[25]
SLM operation	25 k	1.634	0.065 (SLM)	~7.3%	9.8%	[26]
High conversion efficiency	5 k	1.485	0.33	51%	56%	[33]
	5	1.240	9.7	24.5	46%	[38]
High brightness	36 k	1.485	0.45	40%	58.6	[35]
Wavelength expansion	10	3.38–3.80	0.115	18%	—	[31]

red laser is shown in Figure 11. Moreover, the above-mentioned Ref. [22] took advantage of microcavity using a 5-mm-long diamond to achieve an SLM ns-pulsed Stokes output. These three experimental results are arranged in Table 6.

Discussions and conclusion

This paper summarizes the research status of ns-pulsed Raman lasers based on the excellent single-crystal diamond. Due to the high material quality and gain coefficient, near quantum-limit Raman conversion efficiency was achieved and a maximum ns-pulse energy of about 10 mJ at 1.240 μm was reported. As a consequence of the broad transmission window, ns-pulsed DRLs have been demonstrated at wavelengths covering from visible at 0.475 μm to NIR at 1.240 μm to MIR at 3.80 μm. The nature of spatial-hole-burning free and beam clean-up make ns-pulsed DRLs suitable for narrow-linewidth output with SLM and bright beam output with near diffraction limit. Monolithic DRL has the advantages of compact integration, robustness and narrow spectral output, so it draws great attention to generate stable ns-pulsed SLM outputs. The representative results of ns-pulsed DRLs are shown in Table 7.

Improving the output power of ns-pulsed laser is an eternal pursuit. Currently, the main limitation of ns-pulsed DRL for power scaling is the available Type IIa diamond crystal dimensions, which are reported to be up to 10 mm^2 ×

$4\ mm^2 \times 2\ mm^2$. The intracavity Raman gain is inadequate due to the short crystal length, and the pulse intensity of the pump and the generated Stokes has been closed to the crystal damage threshold because of the limited beam size inside the diamond crystal. For example, in the case of the pulse duration of 10 ns, the damage threshold of $8\ GW/cm^2$, beam waist of $1\ mm^2$, crystal length of 10 mm and conversion efficiency of 50%, the maximum output energy of 1.240 μm is calculated as 267 mJ. Owning to the excellent thermal properties and beam clean-up effect, diamond is well suited to achieve ns-pulsed output with high pulse energy, high pulse frequency rate and good beam quality. Besides, ns pulsed DRLs have currently concentrated in the visible, NIR and "eye-safe" bands. With the wide transparence, DRL can be easily extended to ultraviolet and MIR region by using frequency doubling, sum and difference frequency, and cascaded Raman shifts. Finally, taking advantage of the no spatial-hole burning effect, high power ns-pulsed DRLs with narrow linewidth and excellent coherence are also promising.

Author contributions

All authors listed have made a substantial, direct, and intellectual contribution to the work and approved it for publication.

Funding

This work is funded by National Natural Science Foundation of China (62005073); Natural Science Foundation of Hebei Province (F2020202026); Program of State Key Laboratory of Quantum Optics and Quantum Optics Devices (No: KF202207).

Conflict of interest

The authors declare that the research was conducted in the absence of any commercial or financial relationships that could be construed as a potential conflict of interest.

Publisher's note

All claims expressed in this article are solely those of the authors and do not necessarily represent those of their affiliated organizations, or those of the publisher, the editors and the reviewers. Any product that may be evaluated in this article, or claim that may be made by its manufacturer, is not guaranteed or endorsed by the publisher.

References

1. Kunimori H, Greene B, Hamal K, Prochazka I. Centimetre precision eye-safe satellite laser ranging using a Raman-shifted Nd:YAG laser and germanium photon counter. *J Opt A: Pure Appl Opt* (2000) 2:1–4. doi:10.1088/1464-4258/2/1/301

2. Gong W, Chyba TH, Temple DA. Eye-safe compact scanning LIDAR technology. *Opt Lasers Eng* (2007) 45:898–906. doi:10.1016/j.optlaseng.2007.01.008

3. Larsson H, Steinvall O, Chevalier T, Gustafsson F, Persson A, Andersson P. Characterizing laser radar snow reflection for the wavelengths 0.9 and 1.5 μ. *Laser Radar Technol Appl X* (2005) 5791:293. doi:10.1117/12.603573

4. Shibayama N, Sato-Tomita A, Ohki M, Ichiyanagi K, Park SY. Direct observation of ligand migration within human hemoglobin at work. *Proc Natl Acad Sci U S A* (2020) 117:4741–8. doi:10.1073/pnas.1913663117

5. Ma Y, Li J, Liang D, Lu X. Nanosecond-pulse high-peak-power circle-focusing laser beam for laser processing, Proceedings of SPIE 4915.1 (2020): 363–367. doi:10.1117/12.482916

6. Becht H, Hubach H, Rech M, Trefzger B, Weispfenning M. Efficient lasers for remote sensing. In Dubinskii M, Post G. *Laser technology for defense and security VI* (2010). 76860D. doi:10.1117/12.850783

7. Kane TJ, Hillman PD, Denman CA, Hart M, Phillip Scott R, Purucker ME, et al. Laser remote magnetometry using mesospheric sodium. *J Geophys Res Space Phys* (2018) 123:6171–88. doi:10.1029/2018JA025178

8. Li T, Fang X, Liu W, Gu SY, Dou X. Narrowband sodium lidar for the measurements of mesopause region temperature and wind. *Appl Opt* (2012) 51: 5401–11. doi:10.1364/AO.51.005401

9. Yang X, Zhang L, Cui S, Fan T, Dong J, Feng Y. Sodium guide star laser pulsed at larmor frequency: Erratum. *Opt Lett* (2017) 42:5149. doi:10.1364/ol.42.005149

10. Guo K, Li Q, Wang C, Mao Q, Liu Y, Zhu J, et al. Development of a single-wavelength airborne bathymetric LiDAR: System design and data processing. *ISPRS J Photogramm Remote Sens* (2022) 185:62–84. doi:10.1016/j.isprsjprs.2022.01.011

11. Kuang S, Burris JF, Newchurch MJ, Johnson S, Long S. Differential Absorption Lidar to measure subhourly variation of tropospheric ozone profiles. *IEEE Trans Geosci Remote Sens* (2011) 49:557–71. doi:10.1109/TGRS.2010.2054834

12. Asaka K, Yanagisawa T, Hirano Y. 1.5-Mm eye-safe coherent lidar system for wind velocity measurement. *Lidar Remote Sens Ind Environ Monit* (2001) 4153:321. doi:10.1117/12.417063

13. Kun X, Shuanghong D, Jun Z, Shumei W, Yongna L, Wang M. External resonator PbWO 4 Raman laser excited by 1064 nm nanosecond laser pulses. 光学学报 (2012) 32:0914003. doi:10.3788/AOS201232.0914003

14. Murray JT, Austin WL, Calmes LK, Powell RC, McLean JW, Bryan EL. 1997, *Intracavity solid state Raman marine transmitters*. in, eds. RM Narayanan JE KalshovenJr., Spie, Washington, United States, 88. doi:10.1117/12.277602

15. Jiang P, Zhang G, Liu J, Ding X, Sheng Q, Yu X, et al. 16.7 W 885 nm diode-side-pumped actively Q -switched Nd:YAG/YVO 4 intracavity Raman laser at 1176 nm. *J Phys D Appl Phys* (2017) 50:465303. doi:10.1088/1361-6463/aa8f2b

16. Mildren RP. Intrinsic optical properties of diamond. In: *Optical engineering of diamond*. New York, United States: Wiley (2013). p. 1–34. doi:10.1002/9783527648603.ch1

17. Granados E, Spence DJ, Mildren RP. Deep ultraviolet diamond Raman laser. *Opt Express* (2011) 19:10857. doi:10.1364/oe.19.010857

18. Ma S, Tu H, Lu D, Hu Z, Jiang N, Wang X, et al. Efficient Raman red laser with second-order Stokes effect of diamond crystal. *Opt Commun* (2021) 478:126399. doi:10.1016/j.optcom.2020.126399

19. Yang X, Kitzler O, Spence DJ, Williams RJ, Bai Z, Sarang S, et al. Single-frequency 620 nm diamond laser at high power, stabilized via harmonic self-suppression and spatial-hole-burning-free gain. *Opt Lett* (2019) 44:839. doi:10.1364/ol.44.000839

20. Mildren RP, Butler JE, Rabeau JR. CVD-diamond external cavity Raman laser at 573 nm. *Opt Express* (2008) 16:18950. doi:10.1364/oe.16.018950

21. Mildren RP, Sabella A. Highly efficient diamond Raman laser. *Opt Lett* (2009) 34:2811. doi:10.1364/ol.34.002811

22. Granados E, Granados C, Ahmed R, Chrysalidis K, Fedosseev VN, Marsh BA, et al. Spectral synthesis of multimode lasers to the Fourier limit in integrated Fabry–Perot diamond resonators. *Optica* (2022) 9:317. doi:10.1364/optica.447380

23. Cai Y, Gao F, Chen H, Yang X, Bai Z, Qi Y, et al. Continuous-wave diamond laser with a tunable wavelength in orange–red wavelength band. *Opt Commun* (2023) 528:128985. doi:10.1016/j.optcom.2022.128985

24. Sabella A, Piper JA, Mildren RP. 1240 nm diamond Raman laser operating near the quantum limit. *Opt Lett* (2010) 35:3874. doi:10.1364/ol.35.003874

25. Wang Y, Peng W, Yang X, Peng J, Sun Y, Ma Y, et al. Efficient operation near the quantum limit in external cavity diamond Raman laser. *Laser Phys* (2020) 30: 095002. doi:10.1088/1555-6611/ab9d76

26. Ma H, Wei X, Zhao H, Zhang M, Zhou H, Zhu S, et al. Nanosecond pulsed single longitudinal mode diamond Raman laser in the 1.6 μm spectral region. *Opt Lett* (2022) 47:2210. doi:10.1364/ol.458424

27. Bai Z, Williams RJ, Jasbeer H, Sarang S, Kitzler O, Mckay A, et al. Large brightness enhancement for quasi-continuous beams by diamond Raman laser conversion. *Opt Lett* (2018) 43:563. doi:10.1364/ol.43.000563

28. Williams RJ, Nold J, Strecker M, Kitzler O, Mckay A, Schreiber T, et al. Efficient Raman frequency conversion of high-power fiber lasers in diamond. *Laser Photon Rev* (2015) 9:405–11. doi:10.1002/lpor.201500032

29. Williams RJ, Kitzler O, McKay A, Mildren RP. Investigating diamond Raman lasers at the 100 W level using quasi-continuous-wave pumping. *Opt Lett* (2014) 39: 4152. doi:10.1364/ol.39.004152

30. Bai Z, Williams RJ, Kitzler O, Sarang S, Spence DJ, Mildren RP. 302 W quasi-continuous cascaded diamond Raman laser at 15 microns with large brightness enhancement. *Opt Express* (2018) 26:19797. doi:10.1364/oe.26.019797

31. Sabella A, Piper JA, Mildren RP. Diamond Raman laser with continuously tunable output from 3.38 to 3.80 μm. *Opt Lett* (2014) 39:4037. doi:10.1364/ol.39.004037

32. Lux O, Sarang S, Williams RJ, McKay A, Mildren RP. Single longitudinal mode diamond Raman laser in the eye-safe spectral region for water vapor detection. *Opt Express* (2016) 24:27812. doi:10.1364/oe.24.027812

33. Sabella A, Piper JA, Mildren RP. Efficient conversion of a 1064 μm Nd:YAG laser to the eye-safe region using a diamond Raman laser. *Opt Express* (2011) 19: 23554. doi:10.1364/oe.19.023554

34. McKay A, Liu H, Kitzler O, Mildren RP. An efficient 14.5 W diamond Raman laser at high pulse repetition rate with first (1240 nm) and second (1485 nm) Stokes output. *Laser Phys Lett* (2013) 10:105801. doi:10.1088/1612-2011/10/10/105801

35. McKay A, Kitzler O, Mildren RP. Simultaneous brightness enhancement and wavelength conversion to the eye-safe region in a high-power diamond Raman laser. *Laser Photon Rev* (2014) 8:37–41. doi:10.1002/lpor.201400012

36. Pashinin VP, Ralchenko VG, Bolshakov AP, Ashkinazi EE, Gorbashova MA, Yurov VY, et al. External-cavity diamond Raman laser performance at 1240 nm and 1485 nm wavelengths with high pulse energy. *Laser Phys Lett* (2016) 13:065001. doi:10.1088/1612-2011/13/6/065001

37. Dziechciarczyk L, Zhu S, Lin D, Hawkins TW, Dong L, Kemp A, et al. 9 W average power, 150 kHz repetition rate diamond Raman laser at 1519 nm, pumped by a Yb fibre amplifier. In: Proceedings of the Conference on Lasers and Electro-Optics Europe & European Quantum Electronics Conference; 23-27 June 2019; Munich, Germany. IEEE (2019). 1–1. doi:10.1109/CLEOE-EQEC.2019.8873181

38. Williams RJ, Kitzler O, Bai Z, Sarang S, Jasbeer H, McKay A, et al. High power diamond Raman lasers. *IEEE J Sel Top Quan Electron* (2018) 24:1–14. doi:10.1109/JSTQE.2018.2827658

39. Kaminskii AA, McCray CL, Lee HR, Lee SW, Temple DA, Chyba TH, et al. High efficiency nanosecond Raman lasers based on tetragonal PbWO4 crystals. *Opt Commun* (2000) 183:277–87. doi:10.1016/S0030-4018(00)00842-7

40. Zverev PG, Basiev TT, Osiko VV, Kulkov AM, Voitsekhovskii VN, Yakobson VE. Physical, chemical and optical properties of barium nitrate Raman crystal. *Opt Mater (Amst)* (1999) 11:315–34. doi:10.1016/S0925-3467(98)00031-7

41. Mildren RP, Sabella A, Kitzler O, Spence DJ, McKay AM. 2013, Diamond Raman laser design and performance. In: *Optical engineering of diamond*. New York, United States: Wiley. p. 239–76. doi:10.1002/9783527648603.ch8

42. Li Y, Ding J, Bai Z, Yang X, Li Y, Tang J, et al. Diamond Raman laser: A promising high-beam-quality and low-thermal-effect laser. *High Pow Laser Sci Eng* (2021) 9:e35. doi:10.1017/hpl.2021.25

43. Balmer RS, Brandon JR, Clewes SL, Dhillon HK, Dodson JM, Friel I, et al. Chemical vapour deposition synthetic diamond: Materials, technology and applications. *J Phys : Condens Matter* (2009) 21:364221. doi:10.1088/0953-8984/21/36/364221

44. Mildren RP. Intrinsic optical properties of diamond. In: *Opt eng diam*. New York, United States: Wiley (2013). p. 1–34. doi:10.1002/9783527648603.ch1

45. Basiev TT, Sobol AA, Zverev PG, Osiko VV, Powell RC. Comparative spontaneous Raman spectroscopy of crystals for Raman lasers. *Appl Opt* (1999) 38:594. doi:10.1364/ao.38.000594

46. Chrysalidis K, Fedosseev VN, Marsh BA, Mildren RP, Spence DJ, Wendt KDA, et al. Continuously tunable diamond Raman laser for resonance laser ionization. *Opt Lett* (2019) 44:3924. doi:10.1364/OL.44.003924

47. Chen Y, Liu J, Zhu X, Wang M, Yang X, Feng Y, et al. Intracavity frequency - doubled pulsed diamond Raman laser emitting at 620 nm. *Appl Phys B* (2022) 128: 186–5. doi:10.1007/s00340-022-07908-6

48. Jelínek M, Kitzler O, Jelínková H, Šulc J, Němec M. CVD-Diamond external cavity nanosecond Raman laser operating at 1.63 μm pumped by 1.34 μm Nd: YAP laser. *Laser Phys Lett* (2012) 9:35–8. doi:10.1002/lapl.201110093

49. Demetriou G, Kemp AJ, Savitski V. 100 kW peak power external cavity diamond Raman laser at 2.52 μm. *Opt Express* (2019) 27:10296. doi:10.1364/OE.27.010296

50. Muye L, Xuezong Y, Yuxiang S, Zhenxu B, Yan F. Single-frequency continuous-wave diamond Raman laser (Invited). *Infrared Laser Eng* (2022) 51: 1–11. doi:10.3788/IRLA20210970

51. Sarang S, Kitzler O, Lux O, Bai Z, Williams RJ, Spence DJ, et al. Single-longitudinal-mode diamond laser stabilization using polarization-dependent Raman gain. *OSA Contin* (2019) 2:1028. doi:10.1364/osac.2.001028

52. Lux O, Sarang S, Kitzler O, Spence DJ, Mildren RP. Intrinsically stable high-power single longitudinal mode laser using spatial hole burning free gain. *Optica* (2016) 3:876. doi:10.1364/optica.3.000876

53. Sun Y, Li M, Mildren RP, Bai Z, Zhang H, Lu J, et al. High-power continuous-wave single-frequency diamond Raman laser at 1178 nm. *Appl Phys Lett* (2022) 121: 141104. doi:10.1063/5.0107200

54. Murray JT, Austin WL, Powell RC. Intracavity Raman conversion and Raman beam cleanup. *Opt Mater (Amst)* (1999) 11:353–71. doi:10.1016/S0925-3467(98)00033-0

55. Chulkov R, Lisinetskii V, Lux O, Rhee H, Schrader S, Eichler HJ, et al. Thermal aberrations and high power frequency conversion in a barium nitrate Raman laser. *Appl Phys B* (2012) 106:867–75. doi:10.1007/s00340-012-4873-4

56. Reilly S, Savitski VG, Liu H, Gu E, Dawson MD, Kemp AJ. Monolithic diamond Raman laser. *Opt Lett* (2015) 40:930. doi:10.1364/ol.40.000930